Available online at www.sciencedirect.com
SCIENCE DIRECT®
Journal of Hydrology 307 (2005) 294–311
Journal of Hydrology
www.elsevier.com/locate/jhydrol

Effect of rainfall and tillage direction on the evolution of surface crusts, soil hydraulic properties and runoff generation for a sandy loam soil

Babacar Ndiaye[1], Michel Esteves*, Jean-Pierre Vandervaere, Jean-Marc Lapetite, Michel Vauclin

Laboratoire d'étude des Transferts en Hydrologie et Environnement (LTHE, UMR 5564, CNRS, INPG, IRD, UJF) BP 53 F-38041 Grenoble Cedex 9, France

Received 29 July 2003; revised 6 October 2004; accepted 25 October 2004

Abstract

The study was aimed at evaluating the effect of rainfall and tillage-induced soil surface characteristics on infiltration and runoff on a 2.8 ha catchment located in the central region of Senegal. This was done by simulating 30 min rain storms applied at a constant rate of about 70 mm h^{-1}, on 10 runoff micro-plots of 1 m^2, five being freshly harrowed perpendicularly to the slope and five along the slope (1%) of the catchment. Runoff was automatically recorded at the outlet of each plot. Hydraulic properties such as capillary sorptivity and hydraulic conductivity of the sandy loam soil close to saturation were determined by running 48 infiltration tests with a tension disc infiltrometer. That allowed the calculation of a mean characteristic pore size hydraulically active and a time to ponding. Superficial water storage capacity was estimated using data collected with an electronic relief meter. Because the soil was subject to surface crusting, crust-types as well as their spatial distribution within micro-plots and their evolution with time were identified and monitored by taking photographs at different times after tillage. The results showed that the surface crust-types as well as their tillage dependent dynamics greatly explain the decrease of hydraulic conductivity and sorptivity as the cumulative rainfall since tillage increases. The exponential decaying rates were found to be significantly greater for the soil harrowed along the slope (where the runoff crust-type covers more than 60% of the surface after 140 mm of rain) than across to the slope (where crusts are mainly of structural (60%) and erosion (40%) types). That makes ponding time smaller and runoff more important. Also it was shown that soil hydraulic properties after about 160 mm of rain were close to those of untilled plot not submitted to any rain. That indicates that the effects of tillage are short lived.

Keywords: Tillage direction; Soil crusting; Rainfall simulation; Tension disc infiltrometer; Ponding time; Senegal

1. Introduction

Infiltration is the process of water penetration through the soil surface. Its evolution during rainfall determines the available water quantity for runoff

* Corresponding author. Fax: +33 476 82 5286.
E-mail address: michel.esteves@hmg.inpg.fr (M. Esteves).
[1] Present address: Département de Génie Civil, Ecole Supérieure Polytechnique, BP A 10 Thiès, Sénégal.

0022-1694/$ - see front matter © 2004 Elsevier B.V. All rights reserved.
doi:10.1016/j.jhydrol.2004.10.016

Nomenclature

A	soil treatment harrowing tillage across the slope ($\perp$)
a	radius of the tension disc infiltrometer (L)
B	soil treatment harrowing tillage along the slope ($\parallel$)
b	parameter (0.55)
C	untilled soil treatment
CR	cumulative rainfall depth since tillage (L)
Cr	runoff coefficient (–)
DEP	depositional crust-type (–)
ERO	erosion crust-type (–)
g	gravitational acceleration (LT^{-2})
I	cumulative infiltration depth (L)
K	soil hydraulic conductivity (LT^{-1})
q	volumetric flux density (LT^{-1})
R	rain intensity (LT^{-1})
RUN	runoff crust-type (–)
S	capillary sorptivity ($LT^{-1/2}$)
SIF	steady-state flux density emanating from the disc infiltrometer (LT^{-1})
SSC	surface water storage capacity (L)
STR	structural crust type (–)
t	time (T)
T_p	ponding time (T)
T_r	time of appearance of flow at the outlet of runoff plots (T)
β	parameter (0.6)
γ	constant (0.75)
θ	volumetric water content (L^3L^{-3})
λ_c	capillary length scale (L)
λ_m	'mean' pore size (L)
ρ_w	specific mass of water (ML^{-3})
σ	water-soil surface tension (MT^{-2})

and for soil moisture to nourish plants between two rains. In dry tropical regions, superficial pellicular features that strongly affect the hydraulic properties of surface horizons mostly control the soil infiltration capacity and consequently, runoff and soil water erosion. In the Sine Saloum region of Senegal, this phenomenon maintains a low level of soil organic matter and hinders all improvements of plant productivity.

In the case of cultivated soils tillage is one of the main factors that strongly modifies surface-soil physical and hydraulic properties (e.g. Burwell et al., 1966; Allmaras et al., 1967) and has a major influence on the hydrology of an agricultural system (Rawls et al., 1980; Ahuja et al., 1998). It affects infiltration by increasing the plough layer porosity (and hence the moisture storage volume and water movement at high water content) and surface roughness (and therefore surface depression storage), and weakens soil structure. However, studies show that tillage effects are not always consistent. For example Logsdon et al. (1990) and Reynolds et al. (1995) reported that tillage disrupted the continuity of pores from the surface. In another study, Logsdon et al. (1993) found that no tillage resulted in faster ponded infiltration rates than did chisel or mouldboard plough. On the other hand, Ankeny et al. (1990) found little impact of tillage on infiltration rates. Meek et al. (1992) showed that tillage between crops increased the infiltration in trafficked soil but decreased the rate or had no effect on non-trafficked one.

Other important aspect of tillage in relation to infiltration is the development of surface crusts which sharply decrease both the infiltration rate and the soil water content and trigger runoff and soil erosion (McIntyre, 1958; Casenave and Valentin, 1992; Bielders et al., 1996, among many others). The crusting in turn is dependent on soil properties, rainfall characteristics and initial soil conditions (Allmaras et al., 1967; Sumner and Steward, 1992).

Tension disc infiltrometers have extensively been used to characterise both soil macroporosity (Watson and Luxmoore, 1986; Wilson and Luxmoore, 1988; Dunn and Phillips, 1991; Everts and Kanwar, 1993; Logsdon et al., 1993; Lin and McInnes, 1995; Mohanty et al., 1996) and hydraulic properties of non-crusted soils (Clothier and White, 1981; Perroux and White, 1988; Smettem and Clothier, 1989; Ankeny et al., 1991; Reynolds and Elrick, 1991; Thony et al., 1991; Vauclin and Chopart, 1992; Logsdon and Jaynes, 1993) as well as of crusted soils (i.e. Vandervaere et al., 1997). Tension infiltrometer

have also been used to determine tillage effects on spatial and temporal variations of soil hydraulic properties. Most field studies have been conducted at the soil surface for one tillage system and for one time (Watson and Luxmoore, 1986; Jarvis et al., 1987; Ankeny et al., 1991; Thony et al., 1991; Everts and Kanwar, 1993; Mohanty et al., 1994, 1996). Other studies have considered different tillage systems (i.e. Ankeny et al., 1990; Sauer et al., 1990; Dunn and Phillips, 1991; Vauclin and Chopart, 1992; Chan and Heenan, 1993; Murphy et al., 1993). A relatively few studies were focused on temporal variations occurring on the soil surface due to weathering (i.e. Mapa et al., 1986; Freebairn et al., 1989; Messing and Jarvis, 1993; Angulo-Jaramillo et al., 1997; Azevedo et al., 1998). Weathering in this context refers to changes in surface characteristics due to rainfall, wetting and drying.

The objectives of the paper are threefold: (i) to describe the influence of tillage and rainfall energy upon infiltration into a sandy loam crusting soil from the central region of Senegal, cumulative rainfall since tillage being used as an index of rainfall energy; (ii) to quantify the resulting evolution of some soil surface hydraulic properties close to saturation, such as capillary sorptivity, hydraulic conductivity, mean characteristic pore size as well as time to ponding, and (iii) to propose an interpretation of the result in light of the surface crusting dynamics.

2. Materials and methods

2.1. Site description

The study consisted in measuring field infiltration using simulated rainfall and tension disc infiltrometry on a range of surface conditions after variable amounts of rainfall since tillage. The experiment was conducted on a sandy loam on the Thysse-Kaymor catchment located in the Senegalese groundnut belt (central part of Senegal). The mean annual rainfall amount is 660 mm with approximately 8 months (October–May) without rain. The mean annual potential evapotranspiration is 2200 mm. Summer corresponds to the rainy season with intense storms and maximum precipitation and runoff. The catchment (2.8 ha) has a very regular slope close to 1%. It presents a slightly incised and rather broad thalweg (Fig. 1a). Soil texture is homogeneous down to 0.2 m depth and correspond to a sandy loam soil with less than 0.5% organic matter at 0–0.1 m (Table 1). In this horizon, the mean bulk density is 1.5 ($\pm$0.07) (g cm^{-3}). The amount of gravel (ranging from 5 to 30% in the first 20 cm) increases with depth to reach 50–60% at 0.45 m where a ferralitic harden layer is present. Soil surface is subject to develop crusting caused by rainfall. The catchment is mainly cropped with groundnut and millet during the rainy season (June–October).

2.2. Experiments description

Three sites (A, B, C) were selected in the catchment (Fig. 1a). Sites A and B (28 m long, 5 m wide, see Fig. 1b) located in a field with groundnut grown during the rainy season 1998 ended in September were conventionally tilled on December with a horse driven harrow to a depth of 7 cm. Tillage was made perpendicular to the slope for site A and along the slope for site B. Site C (Fig. 1a) was selected in a field previously cropped with millet, with no tillage since the harvest in October 1998.

In the following and for the sake of simplicity tillage treatments on sites A and B will be noted, respectively ($\perp$ slope) and ($\parallel$ slope). On both treatments A and B simulated rainfall was applied on plots (1$\times$1 m) bordered by a thin metal sheet driven to a 0.10 m depth. On each treatment, 5 plots labelled N from 1 to 5 received N consecutive simulated rains of about 70 mm h^{-1} during 30 min. Micro-plots 1A and 1B received one rainfall, 2A and 2B received two rainfalls, 3A and 3B received three rainfalls and so on. The time interval between consecutive rainfalls was 1 week which corresponds to the necessary time to dry the soil surface horizon. So, a total of 30 rainfall simulation runs were made for the study. The rainfall simulator was a 4 m high tower equipped with a Laechler nozzle (# 461.008.30) mounted at 3.86 m above the soil surface. For all the experiments the water pressure was maintained constant at 70 kPa and the corresponding sprinkled area was a square of 2 m by 2 m. The amount of rainfall reaching the soil surface was measured with four collecting cans (5.5 cm diameter) located at the four corners of each micro-plot. Runoff was collected

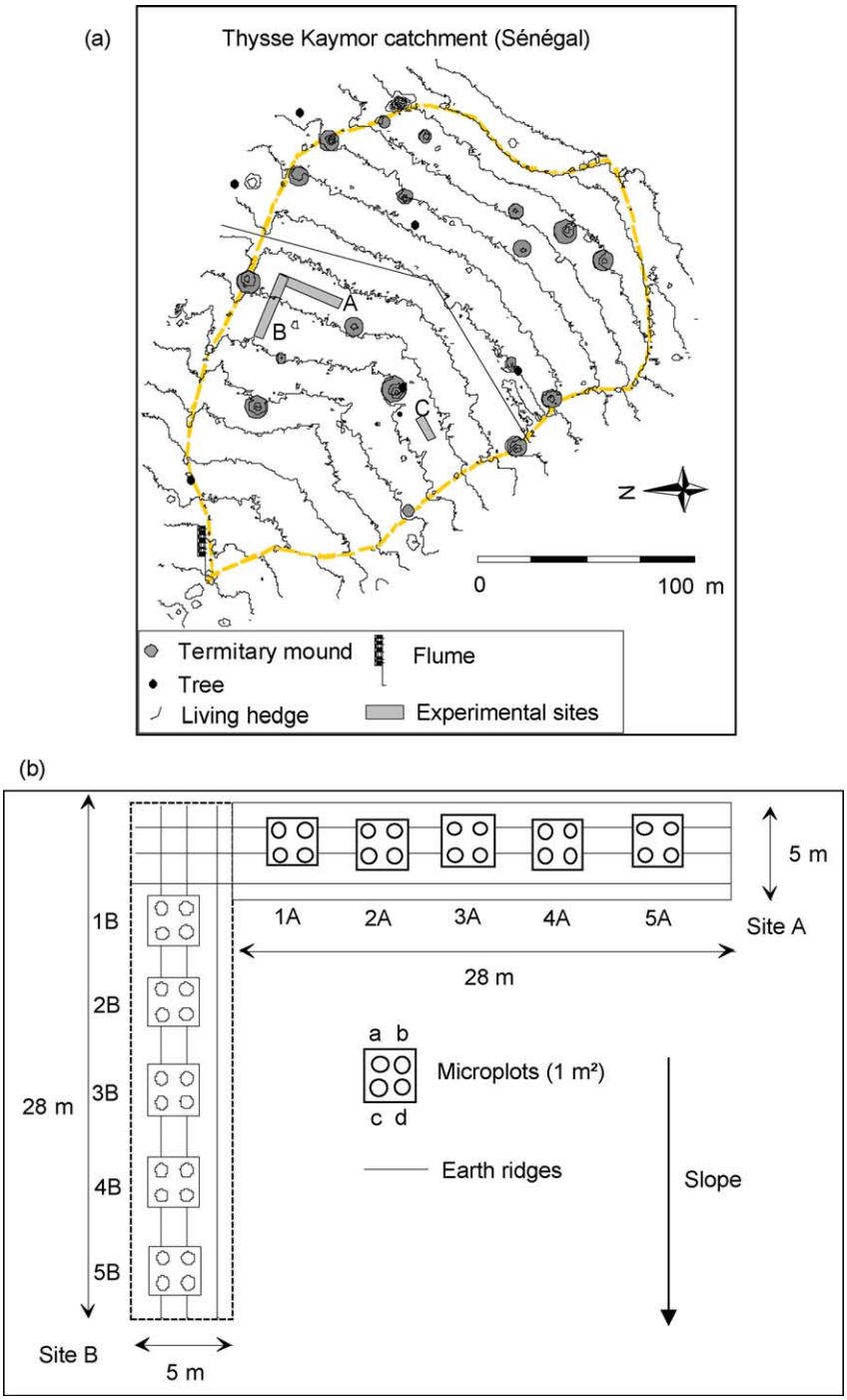

Fig. 1. Schema of the experimental site. (a) Geometry of the 2.8 ha catchment. (b) Location of the runoff micro-plots for treatment A (tillage across the slope) and B (tillage along the slope). Treatment C corresponds to an untilled soil without any rain. Infiltration test were performed on cylinders a, b, c, d.

Table 1
Textural composition (in %) of the soil and the contact sand layer between disc infiltrometer and soil surface

Soil type	Depth	Number of samples	Clay	Fine silt	Coarse silt	Fine sand	Coarse sand
Soil	0–5 cm	21	6.4(0.9)	8.3(0.4)	18.0(0.7)	41.5(0.6)	25.5(1.1)
	5–10 cm	21	7.8(1.0)	9.4(0.6)	18.2(0.6)	40.1(0.7)	24.2(1.0)
Contact material		3	2.9(0.4)	0.6(0.3)	6.6(1.2)	89.7(1.2)	0.9(0.2)

Numbers in brackets indicate one standard deviation.

in a trough at the downstream border of the micro-plot and was measured with a bucket device equipped with a pressure transducer connected to an electronic data recorder.

Before the first rainfall simulation and after each rainfall simulation the micro-relief of the runoff plots was monitored with an electronic relief meter developed by Planchon et al. (2001). Micro-relief was sampled with a 2.5 cm grid resolution. The algorithm described by Planchon and Darboux (2002) was used for calculating the surface water storage capacity (SSC), expressed in mm of water.

In addition, just after the last simulated rainfall, each plot was equipped with four steel cylinders (labelled from a to d, see Fig. 1b) of diameter 23 cm driven into the soil to a depth of 12 cm. Eight such devices were also set up on the untilled site C which did not receive any rain during the experiment.

Tension infiltrometer tests were conducted on each cylinder 1-week after their installation. The disc permeameter of a diameter slightly smaller than the cylinder was basically of the same design as that of Vauclin and Chopart (1992) with automatic recording of the infiltrated water. A sand layer of variable thickness (mean 7 mm) depending on the importance of the micro-relief achieved hydraulic contact between the disc and the soil. The saturated hydraulic conductivity of the contact material is about 450 mm/h and the air-entry pressure value −15 mm. The water pressure imposed at the base of the disc was set up at −0.5 cm of water. As shown in Reynolds and Zebchuk (1996), there is a significant difference between the water pressure at the top and at the basis of a thick sandy contact layer. Considering the thickness of our contact layers, the value of −0.5 cm was sufficient to ensure that no region at the edge of the contact area was at positive pressure head which avoided flow along the cylinder. Soil samples to determine the antecedent water content were collected near each infiltration location beforehand. The disc infiltrometer was placed at the top of each cylinder producing a 1-D infiltration process within the first 12 cm of soil with an axisymmetric lateral extension under that depth. The flux emanating from the disc was recorded until apparent steady state infiltration was achieved. This generally took about 80 min on the average, the longest times being necessary for micro-plots having received the highest amount of simulated rain (i.e. tests 5A and 5B) as well as for site C (more than 150 min). As soon as the monitoring ceased, the disc and the contact sand layer were removed from the surface and soil samples were taken for the determination of water content at depth 0–5 and 5–10 cm.

Prior to these tests, types and spatial distribution of surface crusts present inside the cylinders were estimated by visual inspection as well as by taking colour photographs. Under crop field conditions, morphological degradation of soil surface is related to soil particle displacement by rainfall. In a first stage, the surface is filled in by a structural crust and its infiltrability decreases. When puddles and runoff appear, a second stage takes place, during which depositional crusts are formed. The passage from the 1st to the 2nd stage is related to critical amount of water excess at the soil surface. Following the classification proposed by Casenave and Valentin (1989) for the sahelian zone, the following types of superficial crusts were identified:

- Structural crust (STR) originating from the impact of rain drops;
- Erosion crust (ERO) forming through erosion of the sand layer of structural crusts, following runoff initiation;

- Runoff crust (RUN) resulting from deposition under running water conditions of material eroded from upslope;
- Depositional crust (DEP) corresponding to the sedimentation of particles in still water.

For the RUN and DEP crust types, the deposition occurs on the top of the initial structural crust.

2.3. Infiltration data analysis

Vandervaere et al. (2000a) have shown that the transient regime of axisymmetric infiltration from a tension disc infiltrometer is adequately described by a two-term equation similar to the Philip's (1957) one-dimensional vertical infiltration equation:

$$I = C_1\sqrt{t} + C_2 t \tag{1}$$

where I is cumulative infiltration depth (L), t is time (T).

The coefficients C_1 and C_2 can be represented, as proposed by Haverkamp et al. (1994), by the following expressions:

$$C_1 = S \tag{2}$$

$$C_2 = \frac{2-\beta}{3}K + \frac{\gamma S^2}{a(\theta_0 - \theta_n)} \tag{3}$$

where S is the capillary sorptivity ($LT^{-1/2}$), K is the hydraulic conductivity (LT^{-1}), a is the disc radius (L) and θ is the volumetric water content (L^3L^{-3}). The subscripts n and 0 refer, respectively, to initial and boundary conditions. In Eq. (3) β is a parameter lying in the interval [0,1]. It can be set to 0.6 (Vandervaere et al., 2000b). From comparison with experimental data, Smettem et al. (1994) showed that an appropriate value for γ is a constant equal to 0.75.

All the infiltrometer tests were analysed by the so-called 'Differentiated Linearisation' method (Vandervaere et al., 1997) which was shown to be robust (Vandervaere et al., 2000a). The method consists in differentiating Eq. (1) with respect to $\sqrt{t}$:

$$\frac{dI}{d\sqrt{t}} = C_1 + 2C_2\sqrt{t} \tag{4}$$

and fitting Eq. (4) to the experimental data as a function of $\sqrt{t_i}$; ΔI_i and $\Delta\sqrt{t_i}$ being approximated by finite differences.

The intercept gives an unbiased estimation of sorptivity (Eq. (2)) and the hydraulic conductivity is inferred from the slope of the regression line:

$$K = \frac{3}{2-\beta}\left[C_2 - \frac{\gamma C_1^2}{a(\theta_0 - \theta_n)}\right] \tag{5}$$

The infiltration tests having been performed at the top of cylinders inserted into the soil, the lateral effects (second part of term in bracket of Eq. (5)) has been neglected and K was approximated by:

$$K = \frac{3}{2-\beta}C_2 \tag{6}$$

with $\beta = 0.6$.

As an example, Fig. 2 presents the raw data of an infiltration test (measured flux emanating from the disc infiltrometer and cumulative infiltration) performed on the micro-plot 2A ($\perp$ slope), cylinder b (Fig. 2a) as well as the corresponding relation between $dI/d\sqrt{t}$ and $\sqrt{t}$ (Fig. 2b). The non-linear behaviour of the early time data is due to the effect of the sand contact layer lying between the base of the disc and the soil surface. Such points have been systematically excluded from the analysis of all the experiments. It is worthwhile to note that the behaviour observed in Fig. 2b is quite similar to that theoretically simulated by Vandervaere et al. (2000a) (see their Fig. 2d).

The measured hydraulic properties S and K also allow calculation of a capillary length scale λ_c (L) which can be estimated (Philip, 1985; White and Sully, 1987) by:

$$\lambda_c = \frac{bS^2}{(\theta_0 - \theta_n)(K - K_n)} \tag{7}$$

where b is a parameter taken as $b = 0.55$ (White and Sully, 1987; Warrick and Broadbridge, 1992). The soil prior to the infiltration tests was dry enough to neglect $K_n = K(\theta_n)$.

From λ_c and by using capillary theory, Philip (1985) inferred a 'mean' characteristic pore size λ_m (L):

$$\lambda_m = \frac{\sigma}{\rho_w g \lambda_c} \tag{8}$$

where σ is the surface tension (MT^{-2}), ρ_w is the density of water (ML^{-3}) and g is the gravitational acceleration (LT^{-2}).

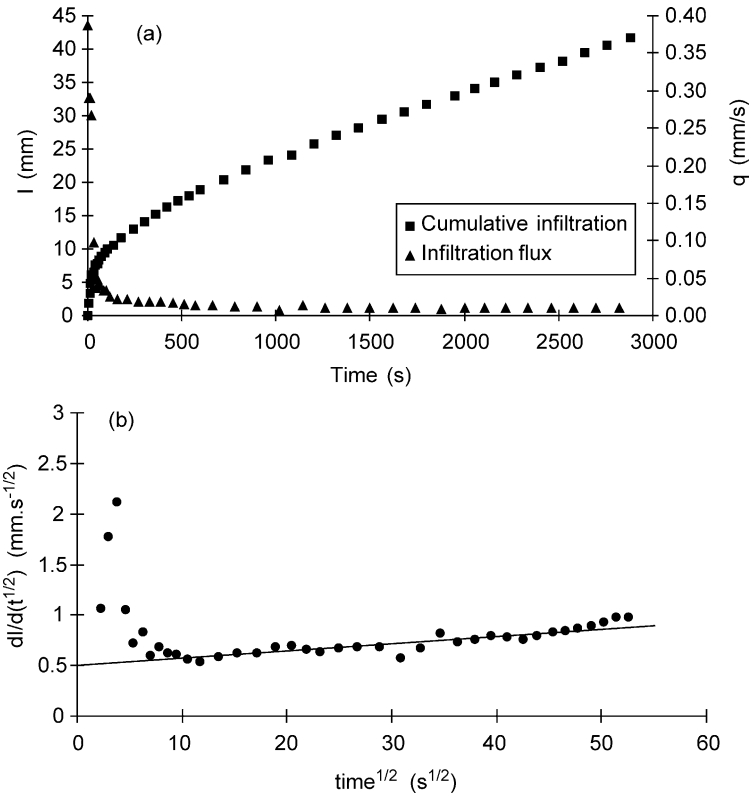

Fig. 2. Example of infiltration test performed on cylinder b of the micro-plot 2A. (a) Raw data of flux (q) and cumulative infiltration (I) as a function of time. (b) Transformed data by the differentiated linearisation method to calculate sorptivity and hydraulic conductivity.

Introducing Eq. (7) into Eq. (8) with $\sigma = 72 \times 10^{-5}$ M m^{-1} at 25 °C leads to:

$$\lambda_m = 13.3 \frac{(\theta_0 - \theta_n)K}{S^2} \tag{9}$$

The larger λ_m, the greater the effect of gravity compared to capillarity, as the infiltration driving force.

Knowledge of sorptivity and hydraulic conductivity close to saturation allows to calculate the time (T_p) for which the soil surface reaches saturation under a constant intensity rainfall (R) greater than the field saturated conductivity. For a hortonian process, all the water infiltrates before T_p and beyond it, only a fraction of the rain enters the soil and the other part accumulates on the surface and/or runs. Boulier et al. (1987) showed that T_p lies between a minimum and a maximum value given respectively by:

$$T_{p_{min}} = \frac{1}{2} \frac{S^2}{RK} \ln\left(\frac{R}{R-K}\right) \tag{10a}$$

$$T_{p_{max}} = \frac{1}{2} \frac{S^2}{R(R-K)} \tag{10b}$$

with $R > K$

When T_{pmin} and T_{pmax} are not too much different the best estimate of T_p was shown to be given by the geometric mean of the two limits (Boulier et al., 1987; Hogarth et al., 1991). In the study we took $T_p = T_{pmax}$ because the rain intensity was only slightly larger than K making T_{pmin} values of the order of tenth of seconds.

The Least Significant Difference Test was used after an analysis of variance to compare the results. Least Significant Difference (LSD) test is a statistical procedure that determines whether the difference

found between two tests is due to the tested effect or the difference is simply due to randomness. For each set of data, a value termed the LSD is calculated at a chosen level of significance. If the difference between the mean of the two tests is greater than this calculated value then it is said to be a 'significant difference' or a difference not due to random chance.

3. Results and discussion

3.1. Simulated rainfall experiments

A total of 30 rainfall simulations were conducted. Table 2 gives their main characteristics as well as the measured runoff values and the times of runoff appearance (T_r) observed for all plots. It summarises the cumulative rainfall (CR) amount applied to the five plots of treatment A ($\perp$ slope) and B ($\parallel$ slope), the mean values of the runoff coefficient (Cr) defined as the ratio between runoff and rainfall depths as well as the mean values of T_r. The influence of cumulative rainfall since tillage viewed as an index of energy (Freebairn et al., 1989) on Cr and SSC are presented in Fig. 3a and b, respectively for both treatments.

The following comments can be made for the mean runoff coefficient: (i) not surprisingly, the runoff coefficients are systematically and substantially higher for treatment B ($\parallel$ slope) than for treatment A ($\perp$ slope). (ii) For both treatments, Cr is an increasing function of CR (at least beyond a threshold of about 65 mm), the rate of increase being higher for B than for A. (iii) While the surface storage capacity (SSC) of the soil harrowed across the slope appears to be quite insensible to the cumulative rainfall, at least up to about 130 mm, tillage along the slope induces a very significant sharp decline of SSC, which can be approximated by an exponentially decaying function of CR as proposed by Zobeck and Onstad (1987) for random roughness ratio and also observed by Freebairn et al. (1989) for chiselling and ploughing treatments. The measurements of surface micro-relief showed that the original micro-topography was smoothed out by infilling up the depressions by sediments detached from the ridges. This process of surface flattening, with cumulative rainfall, occurs faster when the furrows are oriented along rather than across the slope. The runoff coming from upslope causes an additional erosion of the ridges sides. The effect of tillage direction on both Cr and SSC clearly illustrates the role played by runoff on sediments redistribution.

3.2. Relationship between soil surface hydraulic properties and rainfall since tillage

A total of 48 infiltration tests were run to determine the hydraulic properties of the soil surface of the different treatments ($\perp$ slope, $\parallel$ slope and no-tillage). However, due to hydraulic contact problems between the infiltrometer disc and the soil surface, only 43 trials were retained in the analysis. Table 3 gives

Table 2
Rainfall simulations results for treatment A ($\perp$ slope) and B ($\parallel$ slope)

Treatment	Rain number	CR (mm)	Mean Cr (–)	SD Cr (–)	Mean T_r (mn)	SD T_r (mn)
A	R1	34.4	0.13	0.05	23.4	1.2
A	R2	67.0	0.08	0.05	22.8	4.6
A	R3	103.5	0.24	0.10	17.6	3.9
A	R4	140.1	0.29		15.8	
A	R5	178.7	0.34		12.7	
B	R1	40.1	0.29	0.15	14.0	5.7
B	R2	69.1	0.18	0.15	19.7	5.0
B	R3	104.1	0.29	0.25	11.6	2.8
B	R4	138.2	0.39	0.01	11.0	0.3
B	R5	163.3	0.61			

Cr is the runoff coefficient, T_r is the time of appearance of water flow at the outlet and CR is the cumulative rainfall since tillage. SD is the standard deviation.

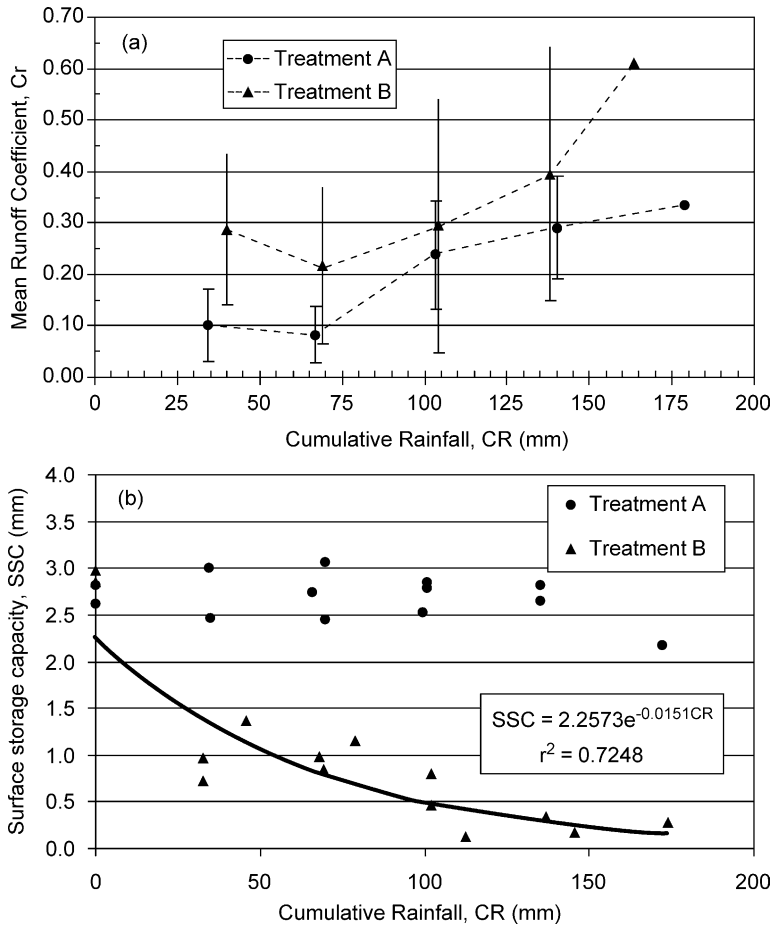

Fig. 3. Runoff coefficient (a) and surface storage capacity (b) as a function of cumulative rainfall since tillage for two treatments. Vertical bars in (a) correspond to ± one standard deviation of the mean values. Line in (b) represents the best fit exponential curve.

the detailed results of each test. The values of S, K, and λ_m were calculated by Eqs. (2), (6) and (9), respectively. Mean values against the cumulative rainfall are plotted in Fig. 4. The results suggest the following comments:

(i) Large standard deviations in S (Fig. 4a) and K (Fig. 4b) reflect important small-scale spatial variability in the pattern of the surface features whatever the tillage treatments and the amounts of rain are.

(ii) For treatment A (⊥ slope) and B (|| slope), soil surface sorptivity close to saturation (S_A and S_B, respectively) decreases with CR (Fig. 4a). The evolution appears to be well described by an exponential function:

$$S_A = 26.5e^{(-3.4\times10^{-3}\ CR)} \text{ with } r^2 = 0.70 \quad (11a)$$

$$S_B = 33.4e^{(-6.3\times10^{-3}\ CR)} \text{ with } r^2 = 0.99 \quad (11b)$$

The decay constant being larger for treatment B (|| slope), making S_B values slightly smaller than S_A ones, at least after the second run of rainfall simulation. The LSD test showed that differences in sorptivities between the two treatments were not significant at the 5% level.

(iii) The same as above are observed for the hydraulic conductivity of both treatments (Fig. 4b).

Table 3
Infiltration tests results. Difference between initial and final soil water content (Delta theta), steady-state flux density (SIF) emanating from the disc, capillary sorptivity (S), hydraulic conductivity (K) and mean pore dimension (Lamda *m*) obtained from 48 runs

Test number (–)	Delta theta (–)	SIF (mm/s)	S (mm h$^{-0.5}$)	K (mm/h)	Lamda m (micron)
1Aa	0.243	0.0079	19.17	65.2	608
1Ab	Experimental problems				
1Ac	0.243	0.0078	23.90	44.8	269
1Ad	0.263	0.0069	18.38	53.8	590
1Ba	0.253	0.0103	27.53	82.4	388
1Bb	Experimental problems				
1Bc	0.261	0.0110	29.48	61.5	260
1Bd	0.237	0.0072	22.47	49.7	328
2Aa	0.247	0.0068	22.22	74.0	522
2Ab	0.224	0.0092	30.09	54.9	191
2Ac	0.286	0.0050	15.23	38.7	672
2Ad	0.261	0.0067	30.03	58.7	239
2Ba	0.190	0.0061	22.54	51.8	274
2Bb	0.203	0.0073	24.59	57.7	273
2Bc	0.286	0.0054	21.10	36.1	327
2Bd	0.293	0.0060	20.39	34.9	346
3Aa	0.250	0.0052	14.57	47.5	790
3Ab	Experimental problems				
3Ac	0.270	0.0081	17.77	59.4	716
3Ad	0.279	0.0083	23.30	57.3	415
3Ba	0.231	0.0040	18.08	7.3	73
3Bb	0.196	0.0046	17.06	34.0	322
3Bc	0.217	0.0098	14.18	27.2	413
3Bd	0.171	0.0044	17.20	15.2	124
4Aa	0.310	0.0068	18.24	42.3	555
4Ab	0.255	0.0058	23.72	43.8	280
4Ac	0.270	0.0059	15.82	49.9	759
4Ad	0.236	0.0043	13.52	36.5	665
4Ba	0.222	0.0025	9.91	20.1	641
4Bb	0.238	0.0042	13.44	31.1	579
4Bc	0.245	0.0019	12.34	3.1	71
4Bd	0.235	0.0050	19.64	19.5	167
5Aa	0.217	0.0022	9.45	11.6	398
5Ab	0.234	0.0091	19.33	52.9	468
5Ac	0.231	0.0056	13.45	55.4	996
5Ad	0.242	0.0064	12.14	68.1	1577
5Ba	0.249	0.0027	16.35	7.8	102
5Bb	Experimental problems				
5Bc	0.233	0.0027	12.27	21.7	472
5Bd	0.213	0.0014	6.24	12.5	964
Ca	0.272	0.0035	14.19	65.9	1251
Cb	0.253	0.0032	19.21	13.3	128
Cc	0.273	0.0051	18.14	29.9	349
Cd	0.272	0.0029	18.12	17.9	210
Ce	Experimental problems				
Cf	0.285	0.0128	30.47	97.2	420
Cg	0.252	0.0027	28.46	68.9	301
Ch	0.253	0.0062	18.73	28.8	293

The rate of decrease is more important for treatment B ($\parallel$ slope) (mean values of K_B varying from about 65 to 14 mm h^{-1}) than for A ($\perp$ slope) for which K_A just declines from about 55 to 48 mm h^{-1}. Application of the LSD test to these results showed that differences in hydraulic conductivities between the two treatments were significant at the 5% level after

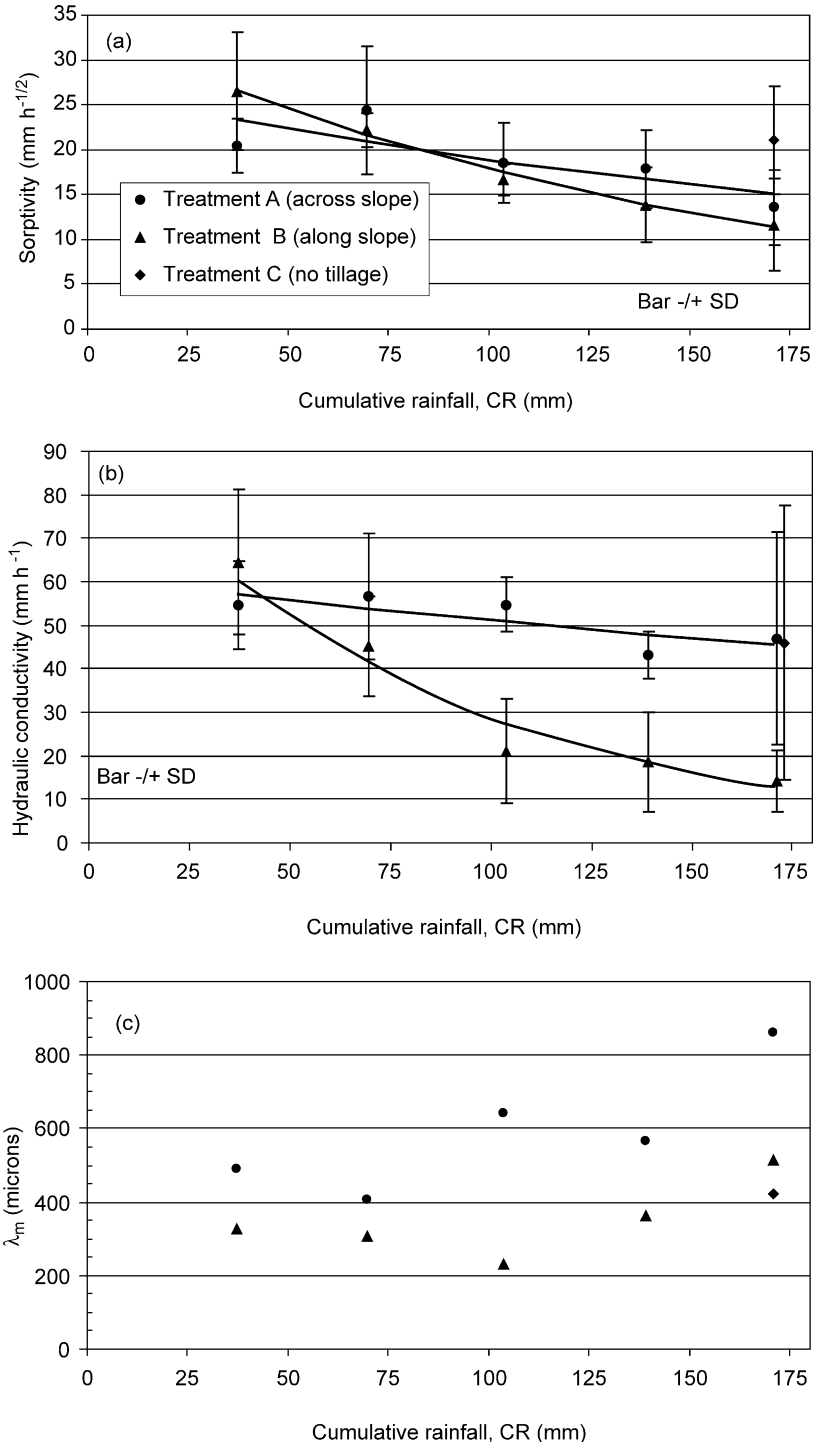

Fig. 4. Soil hydraulic properties as a function of cumulative rainfall since tillage for the three treatments. (a) Sorptivity; (b) hydraulic conductivity; (c) 'mean' pore size. Lines of (a) and (b) represent the best fit exponential curves Eqs. (11a), (11b), (12a) and (12b)). Vertical bars correspond to $\pm$ one standard deviation of the mean values.

a cumulative rainfall of 100 mm. This supports the findings of Rao et al. (1998) who observed the same evolutions and differences on an Indian crusting soil of the same type submitted to similar climatic conditions as encountered in our study. As for sorptivities, the variations of hydraulic conductivities with CR can be approximated by exponential functions, a better fit being obtained for the K_B values:

$$K_A = 60.9e^{(-1.7\times10^{-3}\ CR)} \quad \text{with } r^2 = 0.61 \tag{12a}$$

$$K_B = 93.2e^{(-1.17\times10^{-2}\ CR)} \quad \text{with } r^2 = 0.94 \tag{12b}$$

(iv) Values of S and K for the no-tilled (site C, see Fig. 1) and treatment A ($\perp$ slope) are close to each other. That indicates that the effect of conventional tillage ($\perp$ slope) on infiltration is no more significant after receiving a cumulative rainfall of 163 mm. These evolutions are in agreement with the findings of Mwendra and Feyen (1993) who showed that infiltration into freshly tilled soils was best described by exponentially decaying functions in which surface conditions and properties, rather than profile, control the infiltration process.

(v) On the contrary, the 'mean' characteristic pore size λ_m increases with cumulative rainfall, both the values and the rates of increase being larger for the treatment A ($\perp$ slope) than for the B ($\parallel$ slope) one (Fig. 4c). This indicates that the gravity effect (as compared to the capillarity effect) on the infiltration would be more important for the former than for the latter treatment.

This result is well consistent with the results given in Fig. 4a and b.

Introducing Eqs (11a), (11b), (12a) and (12b) into Eq. (9) gives the following relations:

$$\lambda_A = 277e^{(5.1\times10^{-3}\ CR)} \tag{13a}$$

$$\lambda_B = 267e^{(0.9\times10^{-2}\ CR)} \tag{13b}$$

(λ_A and λ_B are in μm) which are plotted in Fig. 4c. They fit reasonably well, especially for treatment B, the λ_m values obtained straightforwardly by using Eq. (9) alone. Eqs. (13a) and (13b) show that, just before the first rain simulation (CR = 0), soil of treatments A ($\perp$ slope) and B ($\parallel$ slope) are characterised by the same value of λ_m. Also, it may be noted that the values are of the same order of magnitude as those reported in White and Sully (1987) for several field soils and that the increase of λ_m has not yet been clearly understood.

In addition it is worthwhile to mention that mercury porosimetry was performed on a soil clod taken close to the soil surface of treatment A ($\perp$ slope) after about 170 mm of rain was applied. The results showed a bimodal pore size distribution with the first peak at 3×10^{-2} μm and the second around 40 μm, 80% of the pore size cumulative probability distribution lying between 2 and 400 μm (Ndiaye, 2001) which is smaller than λ_m. Once again (White and Sully, 1987) it appears that mercury porosimetry method is doubtful to estimate the dimension of pores, which are hydraulically functioning in field conditions.

3.3. Ponding time

Fig. 5 presents the values of T_p as a function of CR for treatment A ($\perp$ slope) and B ($\parallel$ slope). They were calculated by Eq. (10b) with the values of the observed rainfall intensities (Table 2). S and K being obtained from the infiltration tests (see Fig. 4a and b, respectively). For comparison purposes, the observed values of T_r (see Table 2) are also reported. Not surprisingly, T_p decreases as CR increases, the values being larger for treatment A than for treatment B, that is fully consistent with the previous results dealing with the behaviour of S and K. In addition they are in fair agreement with T_r, by realising that T_r corresponds to the time at which the runoff flow was first detected at the outlet of the 1 m^2 plots, while T_p is the time at which the soil surface reaches saturation (in fact the pressure head of −5 mm of water, imposed at the base of the disc infiltrometer). As a matter of fact, the difference $T_r - T_p$ (about 9 min) can be seen as the time needed first to fill in the superficial storage capacity of the surface (about 4 min for treatment A; from 4 to 1 min for treatment B) and second, to establish the continuity of water pathways at the surface, which is required before water runs outside

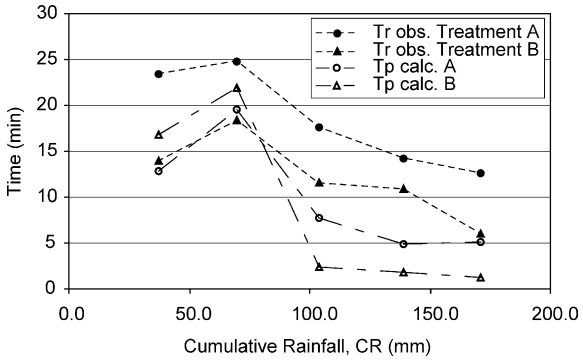

Fig. 5. Calculated ponding time (T_p) and observed time of appearance of runoff (T_r) as a function of cumulative rainfall since tillage for two treatments.

the plots. Of course, those two processes depend upon the time evolutions of both micro-topography and crust types, which are quite different between treatments, as it is shown in the following. That is why, it is believed that this agreement is an indicator of correctness of field estimates of hydraulic properties.

Note that the increase of both T_p and T_r (and S as well) between the first and second run of rain simulation has not yet been fully explained.

3.4. Correspondence between distribution of soil crust types and hydraulic properties

Visual evidence for the importance of the role played by soil crusting on infiltration and runoff was provided by taking photographs of the soil surface at different times after tillage. As an example, Fig. 6 pictures the surface feature of plot 5 located on treatment A, before the first rain (a) and after CR = 100 mm (b). Immediately after tillage one can see that the micro-relief is organised in ridges and furrows making the surface rough and that the soil is constituted of clods improving macroporosity. Under the raindrop impact, the ridges and furrows become smoother and smoother as cumulative rainfall increases and because the soil is subject to surface crusting, superficial pellicular features appear and develop. That is clear from Fig. 6b which shows that the ridges and furrows still remain visible, but with the presence of crusts organised according to the genetic model proposed by Bielders et al. (1996): the structural (STR) and erosion (ERO) crusts are present on ridges, runoff (RUN) and depositional (DEP) ones are observed in furrows.

Observed time evolutions of the spatial distribution of the surface crust types (expressed as the percentage of cover) are detailed in Figs. 7 and 8 for treatment A and B, respectively. Also are reported the corresponding measured values of hydraulic conductivity, sorptivity and λ_m. Clearly the results show that tillage direction has a strong influence on the dynamics of crust types as the cumulative rainfall increases and consequently on the surface soil hydraulic properties at least such as inferred by disc infiltrometry. They suggest the following comments:

(i) For CR smaller than 100 mm most of the crust are of STR type on both treatments, a small

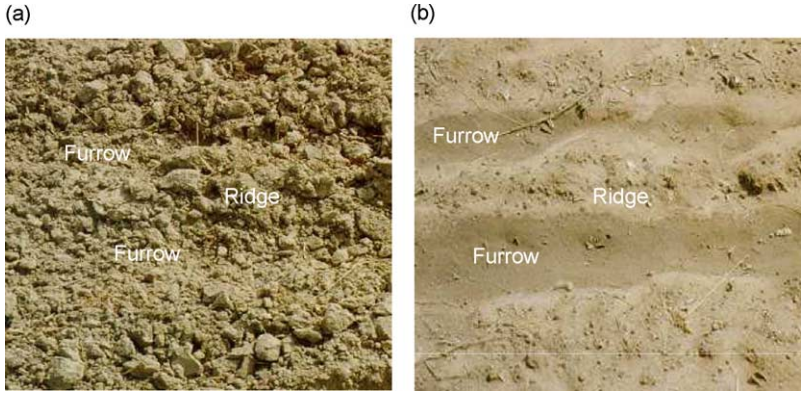

Fig. 6. Views of the surface of a micro-plot taken immediately (a) after harrowing the soil across the slope and (b) after a cumulative rainfall of 100 mm.

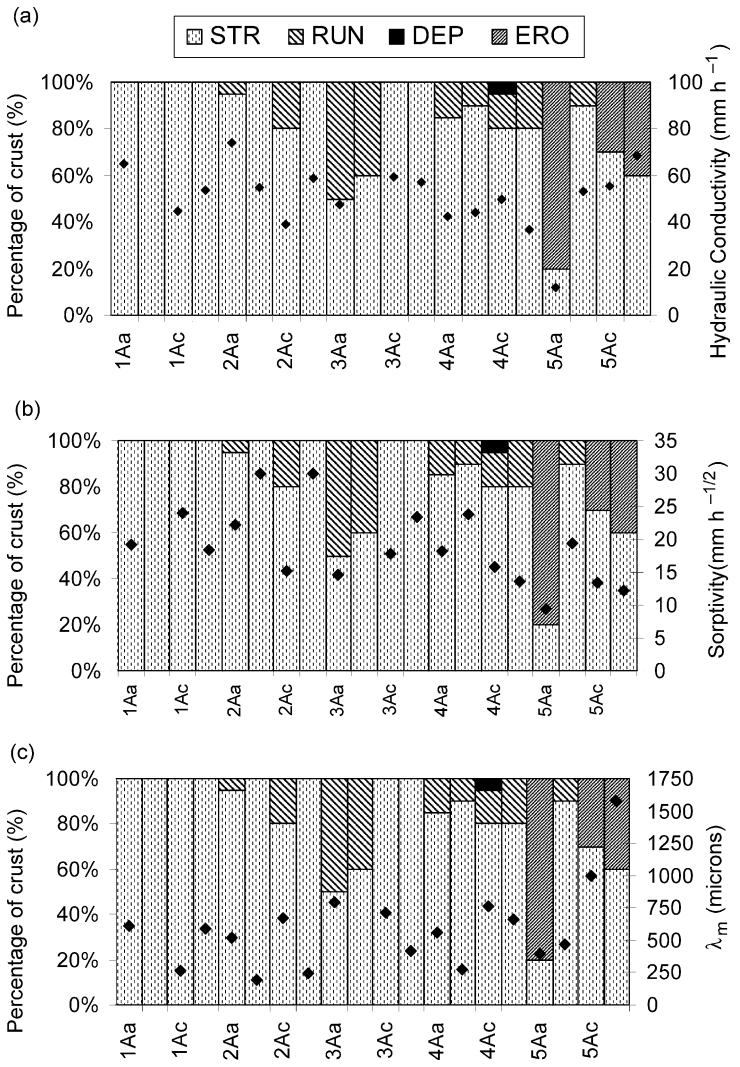

Fig. 7. Correspondence between the percentage of surface crust-types and (a) hydraulic conductivity (K), (b) sorptivity (S) and (c) 'mean' pore size (λ_m) as a function of the number of rains for tillage treatment A (harrowing across slope). Symbols correspond to the measured values of K, S and λ_m.

proportion (about 15%) of depositional one being nevertheless observed on treatment B (|| slope). This is corroborated by the smoothing of the micro-relief (see Fig. 3b) that induces a greater runoff coefficient than on treatment A (⊥ slope) (see Fig. 3a) and a higher rate of deposition of fine particles in depressional areas. The progressive flattening of the micro-topography was also reported in other studies (e.g. Freebairn et al., 1989; Fox et al., 1998a).

(ii) For $100 < CR < 140$ mm, one observes the formation of a significant amount of RUN crusts on treatment A (⊥ slope) (45%) and of ERO crusts on treatment B (|| slope) (60%) which leads to an important decrease of soil hydraulic conductivity for that treatment. That is supported by the findings of Valentin and Bresson (1992) who mentioned that STR crusts may evolve into ERO ones when the washed surface is eroded by both splash and runoff. The same trend is observed on

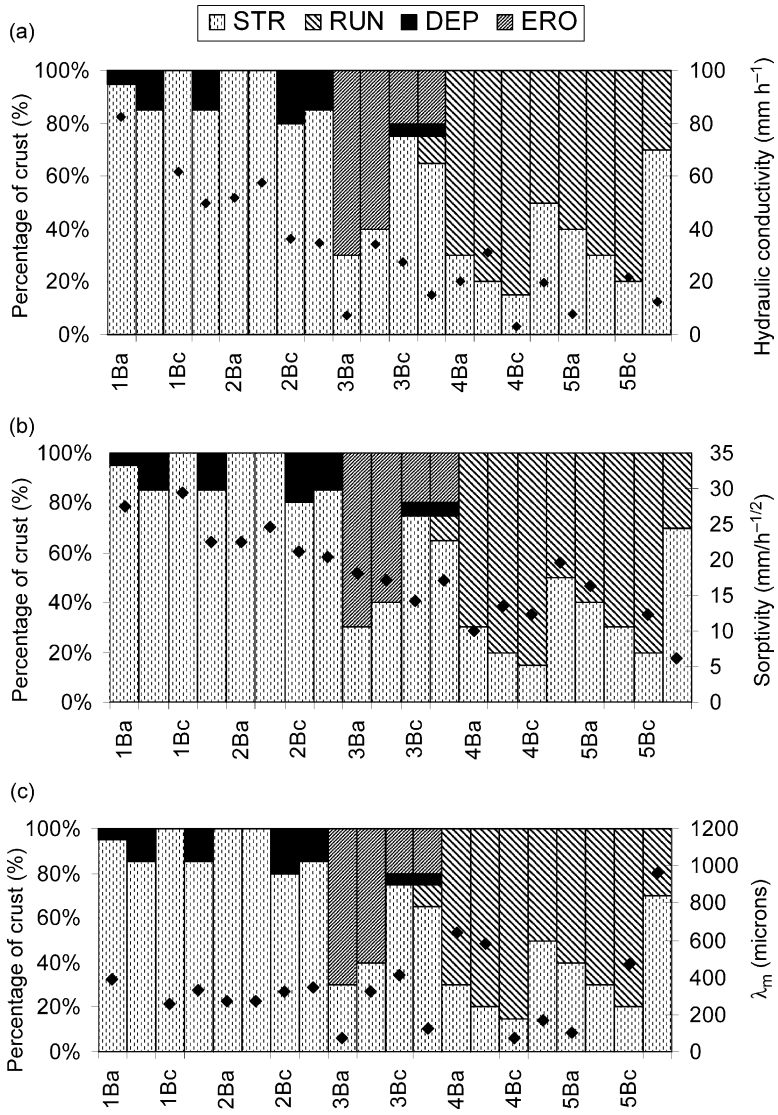

Fig. 8. Correspondence between the percentage of surface crust-types and (a) hydraulic conductivity (K), (b) sorptivity (S) and (c) 'mean' pore size (λ_m) as a function of the number of rains for tillage treatment B (harrowing along slope). Symbols correspond to the measured values of K, S and λ_m.

treatment A ($\perp$ slope), but with a lag delay of about 60 mm of rain.

(iii) For CR > 140 mm, while the presence of the STR crusts appears to be still dominant on treatment A ($\perp$ slope); a very large amount (80%) of RUN crusts take place on treatment B ($\parallel$ slope). The longer persistence of the micro-relief on the former (Fig. 3b) probably maintains higher infiltration rates than on the latter one (Fig. 4a and b), due to increased depth of ponding and greater hydraulic head gradient, while maintaining a higher conductivity. That is well highlighted by greater values of λ_m (Fig. 4c) and smaller value of ponding times (Fig. 5) for treatment A than for treatment B.

(iv) As cumulative rainfall increases, the differentiation between treatment becomes more and more obvious. Within a given treatment the small-scale spatial variability of crust types tends to increase as well. That was also observed by Fox et al. (1998b) who found that seal characteristics vary considerably within a range of a few centimetres.

4. Conclusions

Aside from the clear demonstration that surface crusting does occur in a sandy loam field soil under conditions encountered in the central region of Senegal, it appears to have a very significant impact on the hydrologic properties depending on tillage treatments. Time variations of the infiltration parameters (capillary sorptivity and hydraulic conductivity) with cumulative rainfall since tillage (viewed as an index of rainfall energy) were explained by the crust-types and their temporal dynamics of formation which both were found different according to tillage direction: harrowing either along or across the catchment slope. On the former case (treatment B), the fast development and the large abundance of runoff crusts (resulting from deposition of fine particles eroded from upslope) drastically reduce infiltration rates, making ponding time values smaller and runoff ones larger than those observed when the soil is harrowed across the slope. For the latter (treatment A), structural crusts (originating from the impact of rain drops) and to a lesser extent erosion crusts (formed by erosion of the sandy component of structural crusts, at the initiation of runoff) are dominant and have smaller impact on the reduction of the soil infiltrability.

Surface crust-types were tentatively characterised by the concept of 'mean' pore sizes hydraulically active. The results show that gravity-driven force (relatively to capillary one) is more important on structural and erosion crusts than on runoff ones. Combined with a longer persistence of the superficial soil water storage capacity, it explains why harrowing a soil subject to crusting across the catchment slope facilitates infiltration and subsequently delays the onset of surface runoff.

In addition, soil surface hydraulic properties of an untilled plot not submitted to any rain were found to be close to those of the conventional treatment plot ($\perp$ slope) after receiving a cumulative rainfall of about 160 mm. That indicates that the effects of tillage are short lived for the conditions encountered in the study.

Acknowledgements

This research was supported by the French National Research Program on Hydrology (PNRH) and the Institut de Recherche pour le Développement (IRD), which are gratefully acknowledged.

References

Ahuja, L.R., Fiedler, F., Dunn, G.H., Benjamin, J.G., Garrison, A., 1998. Changes in soil water retention curves due to tillage and natural reconsolidation. Soil Sci. Soc. Am. J. 62, 1228–1233.

Allmaras, R.R., Burwell, R.E., Holt, R.R., 1967. Plow-layer and surface roughness from tillage as influenced by initial porosity and soil moisture of tillage time. Soil Sci. Soc. Am. J. 31, 27–32.

Angulo-Jaramillo, R., Moreno, F., Clothier, B.E., Thony, J.L., Vachaud, G., Fernandez-Boy, E., et Cayuela, J.A., 1997. Seasonal variations of hydraulic properties of soils measured using a tension disc infiltrometer. Soil Sci. Soc. Am. J. 61, 27–32.

Ankeny, M.D., Kaspar, T.C., Horton, R., 1990. Characterization of tillage and traffic effects on unconfined infiltration measurements. Soil Sci. Soc. Am. J. 54, 837–840.

Ankeny, M.D., Ahmed, M., Kaspar, T.C., Horton, R., 1991. Simple field method for determining unsaturated hydraulic conductivity. Soil Sci. Soc. Am. J. 55, 467–470.

Azevedo, A.S., Kanwar, R.S., Horton, R., 1998. Effect of cultivation on hydraulic properties of an Iowa soil using tension infiltrometer. Soil Sci. 163, 22–29.

Bielders, C.L., Baveye, P., Wilding, L.P., Drees, L.R., Valentin, C., 1996. Tillage induced spatial distribution of surface crusts on a sandy paleustult from Togo. Soil Sci. Soc. Am. J. 60, 843–855.

Boulier, J.F., Parlange, J.Y., Vauclin, M., Lockington, D.A., Haverkamp, R., 1987. Upper and lower bounds of the ponding time for near constant surface flux. Soil Sci. Soc. Am. J. 51, 1424–1428.

Burwell, R.E., Allmaras, R.R., Sloneker, L.L., 1966. Structural alteration of soil surfaces by tillage and rainfall. J. Soil Water Conserv. 21, 61–63.

Casenave, A., Valentin, C., 1989. Les états de surface de la zone sahélienne. Influence sur l'infiltration. ORSTOM Ed, Coll. Didactiques, Paris pp. 226.

Casenave, A., Valentin, C., 1992. A runoff capability classification system based on surface features criteria in semi-arid areas of West Africa. J. Hydrol. 130, 231–249.

Chan, K.Y., Heenan, D.P., 1993. Surface hydraulic properties of a red earth under continuous cropping with different management practices. Aust. J. Soil Res. 31, 13–24.

Clothier, B.E., White, I., 1981. Measurement of sorptivity and soil water diffusivity in the field soil. Soil Sci. Soc. Am. J. 45, 241–245.

Dunn, G.H., Phillips, R.E., 1991. Macroporosity of a well-drained soil under no tilled and conventional tillage. Soil Sci. Soc. Am. J. 55, 817–823.

Everts, C.J., Kanwar, R.S., 1993. Interpreting tension-infiltrometer data for quantifying soil macropores: some practical considerations. Trans. ASAE 36, 423–428.

Fox, D.M., Le Bissonnais, Y., Quetin, P., 1998a. The implications of spatial variability in surface seal hydraulic resistance for infiltration in a mound and depression microtopography. Catena 32, 101–114.

Fox, D.M., Le Bissonnais, Y., Bruand, A., 1998b. The effect of ponding depth on infiltration in a crusted surface depression. Catena 32, 87–100.

Freebairn, D.M., Gupta, S.C., Onstad, C.A., Rawls, W.J., 1989. Antecedent rainfall and tillage effects upon infiltration. Soil Sci. Soc. Am. J. 53, 1183–1189.

Haverkamp, R., Ross, P.J., Smettem, K.R.J., Parlange, J.Y., 1994. Three-dimensional analysis of infiltration from the disc infiltrometer. 2. Physical based infiltration equation. Water Resour. Res. 30, 2931–2935.

Hogarth, W.L., Sardana, V., Watson, K.K., Sander, G.C., Parlange, J.Y., Haverkamp, R., 1991. Testing of approximate expression for soil water status at the surface during infiltration. Water Resour. Res. 27, 1957–1961.

Jarvis, N.J., Leeds-Harrrison, P.B., Dosser, J.M., 1987. The use of tension infiltrometer to assess routes and rates of infiltration in a clay soil. J. Soil Sci. 38, 633–640.

Lin, H.S., McInnes, K.J., 1995. Water flow in clay soil beneath a tension infiltrometer. Soil Sci. 159, 375–382.

Logsdon, S.D., Jaynes, D.B., 1993. Methodology for determining hydraulic conductivity with tension infiltrometers. Soil Sci. Soc. Am. J. 57, 1426–1431.

Logsdon, S.D., Allmaras, R.R., Wu, L., Swan, J.B., Randall, G.W., 1990. Macroporosity and its relation to saturated hydraulic conductivity under different tillage practices. Soil Sci. Soc. Am. J. 54, 1096–1101.

Logsdon, S.D., Jordhal, J.L., Karlen, D.L., 1993. Tillage and crop effects on ponded and tension infiltration rates. Soil Tillage Res. 28, 179–189.

Mapa, R.B., Green, R.E, Santo, L., 1986. Temporal variability of soil hydraulic properties with wetting and drying subsequent to tillage. Soil Sci. Soc. Am. J. 50, 1133–1138.

McIntyre, D.S., 1958. Soil splash and the formation of surface crusts by raindrop impact. Soil Sci. 85, 185–189.

Meek, B.D., Rechel, E.R., Carter, L.M., Detar, W.R., Urie, A.L., 1992. Infiltration rate of a sandy loam soil: effect of traffic, tillage and plant roots. Soil Sci. Soc. Am. J. 56, 908–913.

Messing, I., Jarvis, N.J., 1993. Temporal variation in the hydraulic conductivity of a tilled clay soil as measured by tension infiltrometers. J. Soil Sci. 44, 11–24.

Mohanty, B.P., Ankeny, M.D., Horton, R., Kanwar, R.S., 1994. Spatial analysis of hydraulic conductivity measured using disc infiltrometer. Water Resour. Res. 30, 2489–2498.

Mohanty, B.P., Horton, R., Ankeny, M.D., 1996. Infiltration and macroporosity under a raw crop agricultural field in glacial till soil. Soil. Sci. 161, 205–213.

Murphy, B.W., Koen, T.B., Jones, B.A., Huxedurp, L.M., 1993. Temporal variation of hydraulic properties of some soils with fragile structure. Aust. J. Soil Res. 31, 179–197.

Mwendra, E.J., Feyen, J., 1993. Tillage and rainfall effects on infiltration and predictive applicability of infiltration equations. Soil Sci. 156, 20–27.

Ndiaye, B., 2001. Experimental study and modelling of hydrodynamic behaviour of cultivated soils: application to the Thysse Kaymor catchment (Senegal). Thesis Univ. J. Fourier, Grenoble, pp. 183 (in French).

Perroux, K.M., White, I., 1988. Design for disc permeameters. Soil Sci. Soc. Am. J. 52, 1205–1215.

Philip, J.R., 1957. Theory of infiltration: 4. Sorptivity and algebraic infiltration equation. Soil Sci. 84, 257–264.

Philip, J.R., 1985. Reply to "Comments on steady infiltration from spherical cavities". Soil Sci. Soc. Am. J. 49, 788–789.

Planchon, O., Darboux, F., 2002. A fast, simple and versatile algorithm to fill the depressions of digital elevation models. Catena 46, 159–176.

Planchon, O., Esteves, M., Silvera, N., 2001. Micro-relief induced by tillage. Measurement, modelling, and consequences on overland flow and erosion. Catena 46, 141–157.

Rao, K.P.C., Steenhuis, T.S., Cogle, A.L., Srinivasan, S.T., Yule, D.F., Smith, G.D., 1998. Rainfall infiltration and runoff from an Alfisol in semi-arid tropical India. II. Tilled systems. Soil Tillage Res. 48, 61–69.

Rawls, W.J., Onstad, C.A., Richardson, H.H., 1980. Residue and tillage effects on SCS runoff curve numbers. Trans. ASAE 23, 357–361.

Reynolds, W.D., Elrick, D.E., 1991. Determination of hydraulic conductivity using a tension infiltrometer. Soil Sci. Soc. Am. J. 55, 633–639.

Reynolds, W.D., Zebchuk, W.D., 1996. Use of contact material in tension infiltrometer measurements. Soil Technol. 9, 141–159.

Reynolds, W.D., Gregorich, E.G., Curnoe, W.E., 1995. Characterization of water transmission properties in tilled and untilled soils using tension infiltrometers. Soil Tillage Res. 33, 117–131.

Sauer, T.J., Clothier, B.E., Daniel, T.C., 1990. Surface measurements of the hydraulic properties of a tilled and untilled soil. Soil Tillage Res. 15, 359–369.

Smettem, K.R.J., Clothier, B.E., 1989. Measuring unsaturated sorptivity and hydraulic conductivity using multiple disc permeameters. J. Soil Sci. 40, 563–568.

Smettem, K.R.J., Parlange, J.Y., Ross, P., Haverkamp, R., 1994. Three dimensional analysis of infiltration from the disc infiltrometer: 1. A capillary based theory. Water Resour. Res. 30, 2925–2929.

Sumner, M.E., Steward, B.A., 1992. Soil Crusting: Chemical and Physical Processes. Advances in Soil Science. Lewis, Boca Raton, FL.

Thony, J.L., Vachaud, G., Clothier, B.E., Angulo-Jaramillo, R., 1991. Field measurements of the hydraulic properties of soil. Soil Technol. 4, 111–123.

Valentin, C., Bresson, L.M., 1992. Morphology, genesis and classification of surface crusts in loamy and sandy soils. Geoderma 55, 225–245.

Vandervaere, J.P., Peugeot, C., Vauclin, M., Angulo-Jaramillo, R., Lebel, T., 1997. Estimating hydraulic conductivity of crusted soils using disc infiltrometers and minitensiometers. J. Hydrol. 188–189. See also pages 203–223.

Vandervaere, J.P., Vauclin, M., Elrick, D.E., 2000a. Transient flow from tension infiltrometers. Part 1. The two-parameter equation. Soil Sci. Soc. Am. J. 64, 1263–1272.

Vandervaere, J.P., Vauclin, M., Elrick, D.E., 2000b. Transient flow from tension infiltrometers. Part 2. Four methods to determine sorptivity and conductivity. Soil Sci. Soc. Am. J. 64, 1273–1284.

Vauclin, M., Chopart, J.L., 1992. L'infiltrométrie pour la détermination in situ des caractéristiques hydrodynamiques de la surface d'un sol gravillonnaire de Côte d'Ivoire. Agronomie Tropicale 46, 259–271.

Warrick, A.W., Broadbridge, P., 1992. Sorptivity and macroscopic capillary length relationships. Water Resour. Res. 28, 427–431.

Watson, K.W., Luxmoore, R.J., 1986. Estimating macroporosity in a forest watershed by use of a tension infiltrometer. Soil Sci. Soc. Am. J. 50, 578–582.

White, I., Sully, M.J., 1987. Macroscopic and microscopic capillary length and time scales from field infiltration. Water Resour. Res. 23, 1514–1522.

Wilson, G.V., Luxmoore, R.J., 1988. Infiltration, macroporosity, and mesoporosity distributions on two forested watersheds. Soil Sci. Soc. Am. J. 52, 329–335.

Zobeck, T.M., Onstad, C.A., 1987. Tillage and rainfall effects on random roughness. Soil Tillage Res. 9, 1–20.